Microbial diversification is maintained in an experimentally evolved synthetic community.

Zahraa Al-Tameemi[1], Alejandra Rodriguez-Verdugo[1*]

[1] Department of Ecology and Evolutionary Biology, University of California, Irvine, Irvine, CA.

* Corresponding author:

Alejandra Rodríguez-Verdugo

e-mail: alejanr1@uci.edu

Competing interests

The authors declare that they have no conflict of interest.

Running title: Bacterial diversification persists only in a community.

Abstract

Microbial communities are incredibly diverse. Yet, the eco-evolutionary processes originating and maintaining this diversity remain understudied. Here, we investigate the patterns of diversification for *Pseudomonas putida* evolving in isolation and with *Acinetobacter johnsonii* leaking resources used by *P. putida*. We experimentally evolved four experimental replicates in monoculture and co-culture for 200 generations. We observed that *P. putida* diversified into two distinct morphotypes that differed from their ancestor by single-point mutations. One of the most prominent mutations hit the *fleQ* gene encoding the master regulator of flagella and biofilm formation. We experimentally confirmed that *fleQ* mutants were unable to swim and formed less biofilm than their ancestor, but they also produced higher yields. Interestingly, the *fleQ* genotype and other mutations swept to fixation in monocultures but not in co-cultures. In co-cultures, the two lineages stably coexisted for approximately 150 generations. We hypothesized that *A. johnsonii* modulates the coexistence of the two lineages through frequency-dependent selection. However, invasion experiments with two genotypes in monoculture and co-culture did not support this hypothesis. Instead, we found that, at the population level, the two morphotypes coexisted at similar relative abundances in the presence of *A. johnsonii* whereas, in its absence, one of the morphotypes was overrepresented in the population. Overall, our study suggests that interspecies interactions play an important role in shaping patterns of diversification in microbial communities.

Importance

In nature, bacteria live in microbial communities and interact with other species, for example, through the exchange of resources leaked into the external environment (i.e., cross-feeding interactions). The role that these cross-feeding interactions play in shaping patterns of diversification remains understudied. Using a simple bacterial system in which one species cross-feeds resources to a second species (commensal species), we showed that the commensal species diversified into two subpopulations that persisted only when the cross-feeder partner was present. We further observed loss-of-function mutations in flagellar genes that were fixed in monocultures but not in co-cultures. Our findings suggest that cross-feeding species influence patterns of diversification of other species. Given that nutrient leakage is pervasive in microbial communities, the findings from this study have the potential to extend beyond our specific bacterial system. Importantly, our study has contributed to answering the larger question of whether species evolved differently in isolation versus when interacting with other species.

Keywords: interspecies interactions, cross-feeding, evolutionary tradeoffs, maintenance of diversity, experimental evolution, synthetic communities

52 **Introduction**

53 Long-term experimental evolution studies have demonstrated that microbial populations
54 can undergo significant adaptation and diversification over thousands of generations (1). Such
55 adaptation involves the acquisition of new genetic mutations that enhance survival and
56 reproduction in specific environments. Often, these adaptive mutations sweep in the population,
57 resulting in a loss of genetic polymorphism (2, 3). However, polymorphisms are sometimes
58 maintained, leading to the formation of new lineages. For example, in the bacterium *Escherichia*
59 *coli*, acetate specialists evolved from a clonal ancestor that uses glucose and releases acetate as a
60 waste product, resulting in a polymorphic population (4, 5). In addition to cross-feeding, spatial
61 structure can drive microbial diversification by creating distinct ecological niches, which leads to
62 more genetic polymorphism within populations (6-9). For example, during an experiment in
63 static culture conditions, *Pseudomonas fluorescence* diversified into three morphotypes (7).
64 Spatial structure provided an ecological opportunity to types that specialized to the different
65 microenvironments in the flask. Subsequent studies with other species, such as *Burkholderia* and
66 *Bacillus,* have shown that spontaneous diversification due to spatial structure is common (10,
67 11). These studies have also shown that in order to maintain polymorphisms, fitness trade-offs
68 are necessary (12). In addition to fitness trade-offs, negative frequency-dependent selection, in
69 which a rare mutant rises in frequency in a resident population, but loses its fitness advantage
70 when it becomes common, ensures stable coexistence between genotypes (13).

71 In these previous examples, diversification occurs within species, and intraspecific
72 interactions combined with tradeoffs suffice to support polymorphisms (4, 5, 7, 10, 11). Fewer
73 studies have investigated whether other species influence patterns of diversification of species
74 (14). Zhang et al. (2012) showed that the diversification in *P. fluorescence* was not affected by

75 the presence or absence of the competitor species *P. putida*. However, the question of how the
76 presence or absence of a species impacts diversification remains little studied. On the one hand,
77 the presence of other species may limit diversification by reducing the number of niches
78 available for diversification (15). On the other hand, other species may promote diversification
79 given that interspecific interactions promote coexistence within species (16-18). Thus, after
80 polymorphisms have occurred, another species could mediate the coexistence of newly formed
81 lineages. More generally, species interactions alter effective population sizes, which can
82 influence evolutionary processes (19). For example, competitive interactions, which reduce
83 species' population sizes, have been shown to constrain evolution (20). Less is known about what
84 patterns are expected when species interact positively, e.g., when the other species increase their
85 population size. For example, during cross-feeding, microbes exchange metabolites that benefit
86 each other (21). How are patterns of diversification expected to differ when a focal species
87 evolves in isolation compared to when it evolves with another species that cross-feeds resources
88 to it remains an open question.

89 To address this question, we are using a synthetic microbial community composed of
90 *Acinetobacter johnsonii* C6 and *Pseudomonas putida* KT2440. These bacterial species have been
91 isolated from a creosote-polluted aquifer and have naturally evolved to biodegrade aromatic
92 compounds that make up a significant portion of environmental pollutants (22, 23). In addition to
93 its importance for bioremediation, this synthetic community is considered a model system for
94 studying metabolic and commensal interactions (24-26). The commensalism is based on a
95 unidirectional cross-feeding interaction between *A. johnsonii* and *P. putida*. *A. johnsonii*
96 consumes benzyl alcohol and produces benzoate – an intermediate by-product of benzyl alcohol

97 oxidation – which leaks into the external environment where *P. putida* uses it as a source of
98 carbon and energy (27).

99 In this study, we build on a previous evolution experiment in which *P. putida* evolved
100 independently and in conjunction with *A. johnsonii* over 200 generations (28). Over the course of
101 this experiment, we observed that populations of *P. putida* diversified into two morphotypes, but
102 this diversification was maintained exclusively in the presence of *A. johnsonii*. To characterize
103 this diversification, we used both genotypic and phenotypic data to address the following
104 questions: How does trait evolution differ in the presence and absence of *A. johnsonii*? What
105 types of mutations underpin the observed phenotypic diversity? How do these mutations affect
106 physiology and tradeoffs? Finally, what potential processes underly the persistence of this
107 diversity in the co-culture conditions?

108

109 **Materials and Methods**

110 **Growth conditions**

111 All strains were cultured in 10 mL FAB minimal medium (1 mM $MgCl_2$, 0.1 mM $CaCl_2$,
112 0.003 mM $FeCl_3$, 15 mM $(NH_4)_2SO_4$, 33 mM Na_2HPO_4, 22 mM KH_2PO_4, and 50 mM NaCl)
113 with either 0.6 mM of benzoate or 0.6 mM benzyl alcohol as the sole carbon source. The media
114 was run through a 0.2 µm filter and stored in glass treated to remove assimilated organic carbon
115 (AOC). AOC-free glassware was prepared as in Rodriguez-Verdugo et al. (2019) (27). Before
116 running experiments, all strains were acclimated by inoculating 10 µl of frozen glycerol stocks in
117 FAB minimal medium supplemented by either 0.6 mM benzoate or 0.6 mM benzyl alcohol and
118 incubated for 24 hours at 26 °C with constant shaking (150 r.p.m.).

119

120 **Evolution experiment**

121 The evolution experiment had been previously described in Rodriguez-Verdugo and
122 Ackermann (2021) (28). Briefly, the experiment consisted of evolving four replicates of *P.*
123 *putida* in monoculture, four replicates of *A. johnsonii* in monoculture, and four replicates of *P.*
124 *putida* with *A. johnsonii* (i.e., co-cultures) for 30 days, which equates to approximately 200
125 generations (~6.6 generations per day). All cultures were grown in batch culture with FAB
126 minimal media and supplemented with 0.6 mM benzyl alcohol. The experimental lines were
127 established from four ancestors of *P. putida* and *A. johnsonii*, isolated from single clones (Fig.
128 S1). Thus, the ancestors diverged by a few generations when the evolution experiment was
129 started. During the evolution experiment, the population densities for the monoculture and the
130 co-culture from replicate #2 were estimated at the end of each day by plating cultures in LB agar
131 with streptomycin (64 μg/ml) and in LB agar with gentamycin (10 μg/ml) to track *A. johnsonii*
132 and *P. putida*, respectively (28).

133

134 **Growth curves and resource use traits**

135 To characterize the phenotypic diversification of *P. putida* in monoculture and co-culture,
136 we performed growth curve experiments on 30 single colonies isolated from each of the eight
137 experimental lines and from four ancestral populations. Briefly, bacteria were grown in FAB
138 medium supplemented with 0.6 mM benzoate for 24 hours and were then plated on Lysogeny
139 Broth (LB) agar and incubated for another 24 hours at 26 °C. We randomly selected 30 colonies
140 off the plate and resuspended them into wells filled with 200 μL 1% $MgSO_4$ in a 96-well plate.
141 We then transferred 2 μL of the diluted cells and transferred them to another 96-well plate
142 containing 198 μL of FAB supplemented with 0.6 mM benzoate. The plate was sealed with

143 vacuum grease to reduce evaporation. The plate was incubated in a photospectrometer plate
144 reader (Epoch2™, Agilent™) at 30 °C and continuous linear shaking. Optical density (OD)
145 measurements were taken every 10 minutes for 24 hours. From these growth curves, we
146 estimated four quantitative traits involved in resource use: the maximum growth rate in
147 exponential phase (μ_{max}), the yield (Y) defined as the amount of biomass produced per unit of
148 resource, the maximum uptake rate (V) defined as the maximum rate of resource consumption
149 per hour and the half-saturation constant (K) defined as the resource concentration supporting
150 half-maximum uptake rate. Parameters were estimated from growth curves using a multistep
151 approach (27). First, we estimated the yield (in OD/mM) using the formula: $Y = \frac{OD_{max} - OD_{min}}{R_0}$,
152 with OD_{max} being the maximum OD achieved, OD_{min} the minimum OD at the start of the
153 experiment (both in unitless OD), and R_0 the initial concentration of benzoate (= 0.6 mM).
154 Second, we modeled the uptake rate (in mM/OD/h) using the formula: $q = \frac{\mu}{Y}$ where μ is the
155 instantaneous growth rate (h^{-1}) calculated as $\mu = \Delta ln(OD)/\Delta t$. Third, we modeled the change
156 in benzoate over time using the formula: $\frac{dR}{dt} = -\frac{1}{Y}\frac{dP}{dt}$ in which P is the bacterial density (in
157 unitless OD). Finally, we estimated V (in mM/OD/h) and K (in mM) from the function $d(R) =$
158 $\frac{VR}{K+R}$ fitted to the relationship between the uptake rate and the concentration of benzoate.
159 Parameters were fitted to three growth curves (technical replicates) using Matlab (version
160 R2017a, MathWorks). To quantify the evolution of phenotypic traits, we compared the trait
161 distributions from ancestral populations (n = 30) to those from evolved populations (n = 30)
162 using a two-tailed *t*-test (R, version 4.3).
163
164 **Genome resequencing and variant calling**

165 We extracted DNA from the ancestors' clones, monoculture and co-culture populations,
166 and single clones from large and small morphotypes of all four experimental lines. Single clones
167 were revived from glycerol stocks in 3 mL of LB broth and grown overnight at 26 °C with
168 constant shaking (150 r.p.m.). The overnight cultures from monoculture and co-cultures whole
169 populations were grown FAB with 0.6 mM benzoate supplemented with gentamycin (10
170 µg/mL). We isolated and purified genomic DNA from 1 mL of the overnight cultures using the
171 Wizard DNA purification kit (Promega). Short-read sequencing (2 x 150bp paired-end reads)
172 was conducted on a NovaSeq6000 S4 flow cell (UCI Genomics High-Throughput Facility).
173 These sequences can be accessed at the NCBI Sequence Read Archive under Bioproject ID
174 number PRJNA623337.

175 All sequences were aligned to the reference genome of *P. putida* KT2440 (reference
176 NC_002947) using the computational pipeline *breseq* (version 0.36.1) and utility program
177 GDtools (29). We used consensus mode and polymorphism mode to call variants for clones and
178 whole populations, respectively. Each sample was sequenced to a depth of ~600X coverage.
179 Single-nucleotide polymorphisms in genic regions at or above 5% and passing the Fisher's exact
180 test for biased strand distribution were considered. *De novo* non-synonymous mutations were
181 defined as uniquely observed in the evolved sample and not the ancestral clone.

182 Selection and enrichment statistical tests were implemented as in (28). Briefly, the
183 strength of parallelism at the gene level was estimated using a Poisson distribution: $(X = x) =$
184 $\frac{e^{-\lambda}\lambda^{x}}{x!}$ with $\lambda = \frac{\text{total observed mutations}}{\text{genome size in bp}} \times$ size of the target gene in bp. The *P*-value was
185 estimated from the Poisson cumulative expectation, P(x ≥ observed, 1). The cellular functions
186 under selection were determined using the statistical overrepresentation test from Panther
187 (pantherdb.org), version 19.0

188

189 **Physiological tradeoffs**

190 *Biofilm formation* - We measured biofilm formation in the *P. putida* ancestors and the
191 evolved morphotypes using the method described in Martínez-García et al. (2014) (30). Samples
192 were inoculated into FAB media supplemented with 0.6 mM benzoate and incubated for 24
193 hours at 26 °C with constant shaking (150 r.p.m.). The tubes were then vortexed to homogenize
194 the culture and the OD_{600} was adjusted to 0.5. We added 2 µL of the adjusted acclimated culture
195 to a 96-well plate containing 198 µL of FAB and 0.6 mM benzoate and was incubated at 26 °C
196 with no shaking. Each sample was inoculated into 5 wells that serve as technical replicates. After
197 24 hours, the plate was removed from the incubator, and the OD_{600} was measured using the plate
198 reader. The media with planktonic cells was discarded by gently tapping the plate and was
199 washed 3 times with water. The cells attached to the plate were stained by adding 200 µL of
200 0.1% (w/v) crystal violet into each well and were incubated on the bench top for 30 minutes. We
201 then disposed of the crystal violet and gently washed the plate 2-3 times with deionized water.
202 The plate was left to completely dry. We added 200 µL of 33% (w/v) acetic acid to each well,
203 pipetting up and down until it was completely homogenized. The OD_{595} was measured, and an
204 index of biofilm formation was calculated, which was the crystal violet stained biofilm
205 (OD_{595}) divided by the initial culture with planktonic cells (OD_{600}). The higher the biofilm index
206 value, the greater the biofilm formation. These experiments were replicated three times. We
207 conducted a two-tailed *t*-test to determine if there were significant differences in biofilm
208 formation in the evolved morphotypes (n = 3) compared to the ancestor (n = 3).

209 *Motility* - We performed a swimming assay on the ancestors and evolved morphotypes of
210 *P. putida* using 0.3% (w/v) soft agar (30, 31). We inoculated 2 µL of an acclimated culture onto

211 FAB soft agar supplemented with 0.6 mM benzoate and incubated the plates at 30 °C. We
212 measured the halo around the initial inoculum after 24 hours to determine whether the evolved
213 morphotypes' swimming abilities differed from the ancestors' swimming abilities. A larger halo
214 indicates higher motility, while the absence of a halo suggests a lack of flagellar motility.
215

216 **Reciprocal invasion assays**

217 To test if frequency-dependent selection is a possible process for the maintenance of the
218 emergent diversity, we performed reciprocal invasion experiments. These experiments consisted
219 of culturing two morphotypes (large and small) derived from one of the evolved replicates
220 (replicate #2) at a frequency of 5%, 10%, 50%, 90%, and 95% to see if they can invade when
221 rare in the presence and absence of *A. johnsonii.*

222 We used a large and a small clone of *P. putida* (referred as large and small genotypes)
223 from the co-culture #2 isolated at generation 200, which have been genetically characterized in
224 this study (see 'Genome resequencing and variant calling section'). For *A. johnsonii,* we used a
225 single clone from co-culture #2 isolated at generation 200, which was previously sequenced (28).
226 We revived these clones from glycerol stocks by inoculating 10 µl of frozen culture in FAB
227 medium supplemented with 0.6 mM benzoate (for *P. putida*) and with 0.6 mM benzyl alcohol
228 (for *A. johnsonii*) and incubating them at 26ºC with 150 r.p.m. for 24 hours. The OD was then
229 adjusted to 1.0 for both genotypes to standardize the starting ratio. We tested five initial
230 frequencies with a given genotype starting from rare (5%, 10%), equal (50%) or common (90%
231 and 95%). These frequencies were achieved by adjusting the volumetric ratios. For example, for
232 a starting ratio of 10% , 10 µL of the large genotype and 90 µL of the small genotype were
233 inoculated into 9.9 mL of fresh media. For the condition without *A. johnsonii* (i.e., monoculture)

234 the medium was supplemented with 0.6 mM benzyl alcohol. Co-cultures and monocultures were
235 grown at 26°C with constant shaking (150 r.p.m.) for 24 hours. We counted colony-forming
236 units (CFU) at the start of the experiment (T0) and the end of the growth cycle by plating
237 cultures onto LB agar plates supplemented with gentamicin (10 µg mL^{-1}). We included three
238 technical replicates per experiment.

239 The Malthusian parameters for the two genotypes were calculated from cell densities at
240 the initial and final time points, $m = \ln (N_f/N_0)$, with N_0 and N_f the initial and final density after
241 24 hours, respectively. From the Malthusian parameters we estimated the selection rate constant
242 r_{ij} corresponding to the relative growth rate of a morphotype against its competitor. We used the
243 formula $r_{ij} = \frac{m_i - m_j}{1\ day}$ for a pair of competitors *i* and *j* (32, 33). If the value of r_{ij} was
244 significantly larger than zero, the genotype *i* could invade the genotype *j*. If both the large and
245 small genotypes had a positive *r* value when started from rare, the pair was considered to stably
246 coexist through frequency-dependent selection.

247

248 **Evolutionary 'replay' experiment**

249 To better understand the effect of *A.johnsonii* on the maintenance of *P. putida*'s diversity
250 in co-culture, we revived and evolved one of the co-cultures (replicate #2) to see if diversity loss
251 occurred when *A. johnsonii* was removed. We revived co-culture #2 from frozen glycerol stocks
252 stored -80ºC at the 21st transfer day; ~138 generations of evolution. We inoculated 100 µL of the
253 frozen stock into 9.9 mL of FAB with 0.06 mM of benzyl alcohol. In order to remove *A.*
254 *johnsonii* from the community, we added 60 µg/mL of gentamycin to the media and incubated
255 the culture at 26ºC and 150 r.p.m for one day. The removal of *A. johnsonii* was visually
256 confirmed through plating the culture on LB agar plates with streptomycin (64 µg/ml). Two

257 cultures – one *A. johnsonii*-free community and one 'intact' community (control co-culture) –
258 were used to inoculated six culture tubes (technical replicates) with 9.9 mL FAB minimal
259 medium supplemented by 0.6 mM benzyl alcohol. For each daily passage, we transfered 100 µL
260 of culture into 9.9 mL of fresh medium, following the same methodology used for the evolution
261 experiment (28). We did serial transfers for eight days to replay ~ 50 generations of evolution
262 (simulating the last phase of the 200-generations evolution experiment). At the end of a 24-hour
263 growth cycle, we plated 100 µl of culture in LB agar plates supplemented with antibiotics to
264 obtain colony counts.

265

266 **Results**

267 **Phenotypic diversification persisted only in co-culture.**

268 After 200 generations of evolution, we observed diversification of *P. putida* in terms of
269 colony morphology relative to the ancestor (Fig. 1A). All four replicates were bimodal for colony
270 size and consisted of one cluster of strains that formed larger colonies on LB agar plates
271 compared to the ancestor (referred as 'large morphotype'), and one cluster that formed colonies
272 the size of the ancestor (referred as 'small morphotype'). This diversification in colony size was
273 only observed when *P. putida* evolved in co-culture with *A. johnsonii*. In monocultures,
274 populations only formed larger colonies than the ancestor.

275 Next, we quantitively characterized this diversification in four traits involved in resource
276 use. These traits are interdependent – i.e., they all are derived from growth curves – but they
277 provide insights into subtle differences at different phases of the growth cycle. In all monoculture
278 and co-culture replicates, the phenotypic variance for each trait changed compared to the

279 variance of the ancestral population (Figs. S2 and S3). Changes in yield were the most
280 pronounced. We found that *P. putida* grown in co-culture with *A. johnsonii* had a different
281 distribution of yields compared to monoculture (Fig. S2). For example, co-cultures of replicate
282 #2 showed a bimodal distribution, with one subpopulation having a similar yield to the ancestor
283 and the other having a higher yield to the ancestor (Fig. 1B, right panel). On the other hand, the
284 monoculture had a distribution shifted towards higher yield (Fig. 1B, left panel). We confirmed
285 that the large morphotypes previously observed on LB agar plates had higher yields compared to
286 their ancestors, and the small morphotypes had similar yields to their ancestors. For example,
287 large morphotypes from replicate #2 had, on average, a 3.4-fold higher yield than the ancestor
288 (0.068 ± 0.001 and 0.020 ± 0.001 OD per mM for the large and ancestral morphotypes,
289 respectively; t-test, $p < 2.2*10^{-16}$). The small morphotypes achieved a yield of 0.023 ± 0.002 OD
290 per mM, which is comparable to that of the ancestor (t-test, $p = 0.122$).

291 Finally, leveraging the fact that large morphotypes with higher yield formed larger colonies
292 on LB agar plates that could be distinguished from the ancestral morphotype, we tracked the
293 evolution of phenotypic diversification for one of the replicates (replicate #2) during our
294 experiment. After approximately 40 and 70 generations of evolution, we observed the emergence
295 of a large morphotype in monoculture and co-culture, respectively (Fig. 2). In co-culture, the
296 large and small morphotypes coexisted for the remaining 130 generations. Instead, in
297 monoculture, the large morphotype rapidly outcompeted the ancestral morphotype, driving it to
298 extinction after 140 generations. Thus, diversification only persisted in co-culture.

299

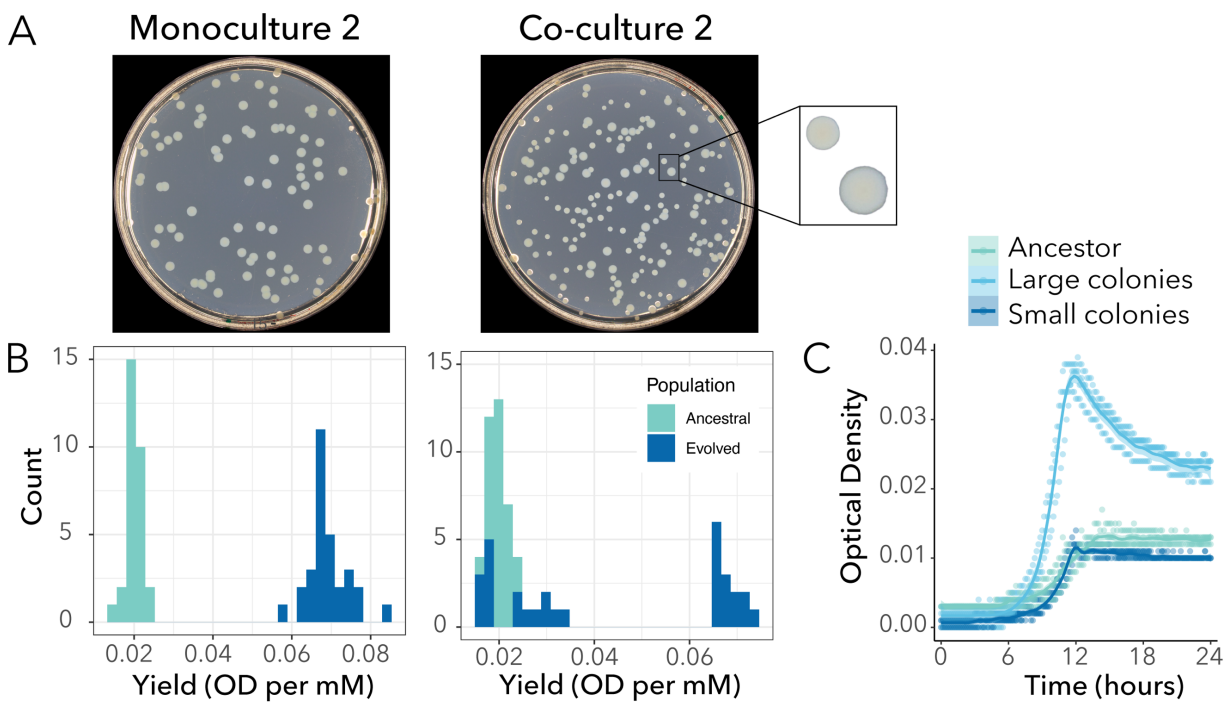

Fig. 1. *P. putida* population evolved in monoculture is monomorphic, while the population evolved in co-culture diversified into two sub-populations after 200 generations. A) Agar plates illustrating the difference in colony morphologies between the evolved population in monoculture (left panel) and the evolved population in co-culture (right panel) for replicate #2. B) Histograms showing the differences in yield distributions between the ancestral and the populations from replicate #2 evolved in monoculture (left panel) and co-culture (right panel). In monoculture, *P. putida*'s population evolved higher yield (t-test, $p < 2.2*10^{-16}$). In co-culture, *P. putida*'s population evolved bimodality (Hartigans' dip test for multimodality, $p < 2.2*10^{-16}$). The results from the other replicates and parameters are available in Fig. S2 and Fig. S3. C) The optical density (OD_{600}) over 24 hours is plotted for three randomly selected colonies (i.e. three replicates) sampled from the ancestral population, the subpopulation forming small morphotypes and the subpopulation forming large morphotypes from co-culture #2.

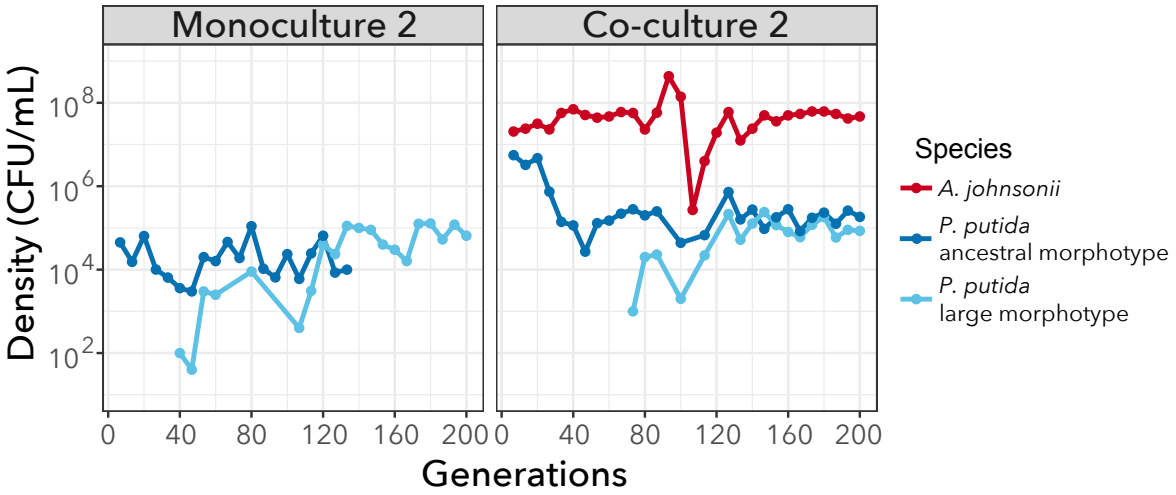

314

315 **Fig. 2. Diversification was maintained in co-culture but not in monoculture.** The large
316 morphotype appears in the monoculture after approximately 50 generations and outcompetes the
317 ancestral morphotype. In co-culture, both morphotypes coexist until the end of the experiment.
318 Population density (CFU mL^{-1}) trajectories from replicate #2 are shown over 200 generations. *A.*
319 *johnsonii*'s densities are from (28). Each point represents the final density of each species and
320 morphotypes after daily cycles of growth; lines connecting circles help visualization and do not
321 have any biological meaning.

322

323 **Morphological diversification in *P. putida* is based on genetic diversification**

324 To determine if the observed phenotypic diversity in the evolved lines (Fig. 1) reflected
325 specific mutations, we performed whole population sequencing to identify *de novo* mutations.
326 Combined, all eight evolved lines accumulated 29 point mutations in open reading frames (Table
327 S1). Most of these mutations were nonsynonymous (nonsynonymous/synonymous ratio = 8.7),
328 indicating a strong signal of adaptive evolution. In additon to point mutations, some lines
329 accumulated short insertions and deletions (<30 bp) and one line had a deletion of 130 bp (Table

330 S1). Mutations targeted functions related to positive regulation of cell motility (GO:2000147),
331 negative regulation of extracellular matrix assembly (GO:1901202), positive regulation of cell-
332 substrate adhesion (GO:0010811), and DNA-template transcription (GO:0006351). There were
333 no differences in total number of mutations in monocultures compared to co-cultures (Fig. 3A).

334 Next, we looked at patterns of convergent evolution. We observed parallel evolution at
335 different levels. The exact same nonsynonymous mutation in the *cmoB* gene was shared among
336 three experimental lines (Table S1). Other mutations also targeted the *cmoB* gene, suggesting it is
337 under strong positive selection. The CmoB enzyme is involved in post-transcriptional
338 modifications of tRNA molecules, but its functional relevance remains underexplored. Another
339 gene repeatedly targeted was the *fleQ* gene, encoding FleQ, a master transcriptional regulator of
340 flagella and biofilm formation. Four out of the eight lines had mutations in the *fleQ* gene. This
341 parallelism suggests this gene is under strong selection based on the expectation that observing
342 four random mutations in a 1476 bp gene is extremely low (Poisson cumulative expectation, $P =$
343 $2*10^{-12}$). More generally, approximately one-third of mutations (including deletions and
344 insertions) targeted the same genes in monocultures and co-cultures, while the rest were either
345 found exclusively in monocultures (~ 43%) or in co-cultures (~ 25%; Fig. 3B). For example,
346 mutations in the *uvrY* gene encoding a UvrY/SirA/GacA family response regulator were
347 observed exclusively in two co-cultures and may be indicative of adaptations to the biotic
348 conditions (presence of *A. johnsonii*). Interestingly, hard sweeps were only observed in
349 monocultures; i.e., two lines evolved in monocultures had mutation fixed in the population (i.e.
350 at a frequency of 100%; Fig. 3C). One of the monocultures (from replicate #2) had a frameshift
351 mutation in the *fleQ* gene fixed in the population (Table S1). The other monoculture (from
352 replicate #4) had two fixed mutations: one frameshift mutation in the *flgH* gene coding for

353 flagellar basal body L-ring protein FlgH and one non-synonymous mutation in the *gacS* gene
354 coding the sensor protein GacS. Mutations in the *fleQ* and *gacS* genes were also observed in co-
355 cultures but were not fixed in the population. For example, mutations in the *fleQ* gene were
356 observed at a frequency of 23.1%, 35.6%, and 7.5% in replicates #1, 2 and, 4, respectively.

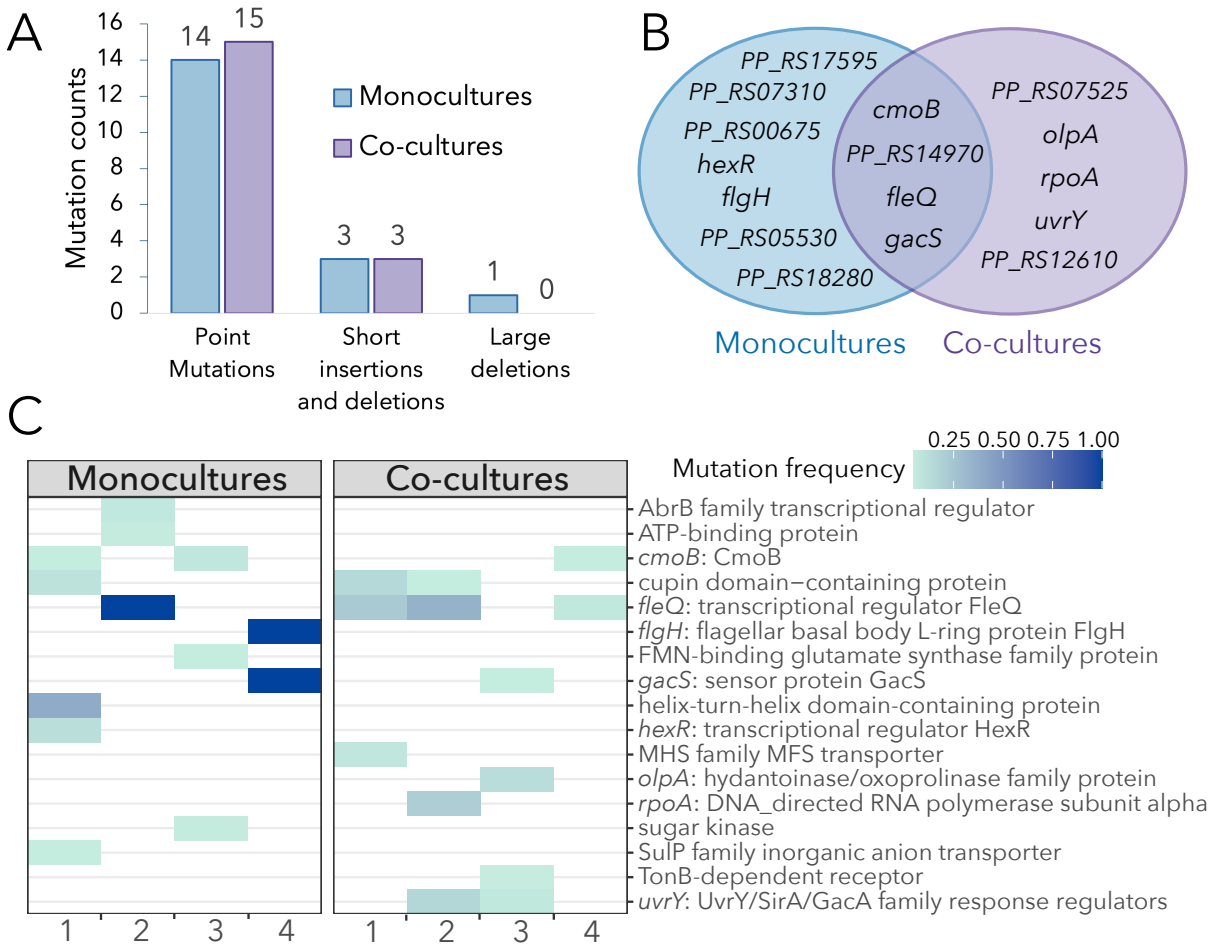

357

358 **Fig. 3. Mutational landscape of monocultures compared to co-cultures**. A) Mutations count
359 according to types: point mutations (both synonymous and non-synonymous mutations), short
360 insertions or deletions (i.e. short in-frame indels), and large deletions (>30 bp). B) Venn Diagram
361 showing convergence of mutations in genes. C) Heat map showing the frequency of non-
362 synonymous mutations (genes = rows) in four monocultures and four co-cultures (columns).

363 Genes with mutations at frequencies above 0.05 are shown. The frequency of each mutation is
364 shown by different intensities of blue: darker blue corresponds to mutations at higher
365 frequencies.

366

367 Finally, we investigated the linkage of these mutations within single clones that formed
368 large morphotypes (from monoculture and co-culture conditions) and small morphotypes (from
369 co-cultures). In average each clone had one mutation, although some clones had two or no
370 mutations (Table 1). Three out of four small morphotypes had one non-synonymous mutation.
371 Thus, despite having a similar yield to the ancestor, they differed from it by one mutation. Most
372 of these mutations were present at low frequency in the population (< 5 %) and affected
373 unanotated genes. One exception was the small morphoptype from replicate #3, which had a 1 bp
374 deletion in the *oplA* gene and was present at a 12.9% frequency in the population (Table S1). The
375 *oplA* gene codes for 5-oxoprolinase A, which has been associated with the catabolism of amino
376 acid derivatives (34, 35) and surface attachment abilities (36). Instead, the large morphotypes
377 were often associated with high frequency mutations in the *fleQ*, *flgH* and *gacS* genes. Notably,
378 two of these large morphotypes were single mutants; i.e. they had only one *fleQ* mutation in the
379 ancestral background (Table 1). Thus, their higher yield compared to the ancestor could be
380 directly attributed to the effect of the mutation. That said, two of the large morphotypes had no
381 mutations in coding regions but had mutations in intergenic regions. It is possible that these
382 mutations are associated to promoters but the genetic bases for their higher yield requires futher
383 investigation.

384 Taken together, we identified the *fleQ*, *flgH* and *gacS* mutations as putative adaptive
385 based on the following: 1) they were present at high frequency in the populations (e.g. some

386 were fixed), 2) they displayed high level of parallelism, notably *fleQ*, and 3) single mutants had

387 higher yied compared to the ancestor.

388

389 **Table 1. Frequency of *de novo* mutations in single clones of *P. putida* in monoculture and co-**

390 **culture after 200 generations.** Monoculture data are extracted from our previous study (28);

391 co-culture data were generated in this study.

Clone	Morph.	Position	Mutation	Gene	Freq. in pop.	Description
Mono. 1	Large	3,987,060	Δ1,094 bp	*oplB* / *oplA*	< 5%	-
Mono. 2	Large	4,964,741	2 bp→ C †	*fleQ*	100%	FleQ
		5,715,528	N65N	*tatB*	100%	TatB
		6,029,059	A134A	*kauB*	100%	KauB
Mono. 3	Large	-	-	-	-	-
Mono. 4	Large	1,843,830	D322H	*gacS*	100%	sensor protein GacS
		4,978,570:1	+C	*flgH*	100%	flagellar L-ring protein
Co-culture 1	Large	4,964,681	A226V	*fleQ*	23.1%	trancriptional regulator FleQ
Co-culture 1	Small	-	-	-	-	-
Co-culture 2	Large	4,964,300	L353Q	*fleQ*	35.6%	trancriptional regulator FleQ
Co-culture 2	Small	3,990,098	V128G	PP_RS18280	< 5%	helix-turn-helix domain-containing protein
Co-culture 3	Large	4,635,453	Y101*	*uvrY*	< 5%	UvrY/SirA/GacA family response regulator transcription factor
Co-culture 3	Small	3,987,689	Δ1 bp	*olpA*	12.9%	hydantoinase/oxoprolinase family protein
Co-culture 4	Large	-	-	-	-	-
Co-culture 4	Small	4,025,185	A172T	PP_RS18445	< 5%	HlyD family efflux transporter periplasmic adaptor subunit

392 † Deletion of first base and substitution of second base with C.

393

394 **Putative adaptive mutations are associated with loss of motility and biofilm formation**

395 In the previous section, we identified putative adaptive mutations in flagellum genes (two
396 of them frameshift mutations). Previous studies have suggested that loss-of-function mutations in
397 flagellar genes are adaptations to the shaking culture conditions. This is because inactivating
398 flagellar motility (which is not necessary in well-mixed environments) saves energy that can be
399 allocated to other cellular functions, e.g., building biomass (30). To test this hypothesis, we
400 explored the mutants' abilities to swim and form biofilms. The motility assay showed a complete
401 lack of motility in the *fleQ* mutants compared to their ancestors (Fig. 3). The large morphotype
402 with mutations in *flgH* and *gacS* also had a reduction in swimming. The other large morphotypes
403 with mutations in genes other than flagellum genes retained the ability to swim. This suggests
404 that their advantages are related to other traits that do not involve flagellar motility. Conversely, a
405 clone from co-culture #4, which formed a small morphotype, lacked motility. This small
406 morphotype had a non-synonymous mutation in the gene PP_RS18445 encoding the HlyD
407 family efflux transporter periplasmic adaptor subunit (Table 1). Therefore, mutations in genes
408 other than flagellum genes can affect motility as well.

409 Mutations in flagellar genes were also associated with a significant reduction in biofilm
410 formation (Fig. 4). The *fleQ* mutants isolated from co-cultures #1 and #2, and monoculture #2,
411 exhibited significant reductions in biofilm formation compared to their ancestors (t-test, p-values
412 of 0.003, 0.023, and 0.008, respectively). The *flgH* mutation (large morphotype from
413 monoculture #4) also had reduced biofilm formation but the difference was marginally
414 significant (t-test, $p = 0.068$).

415 In conclusion, these results support the hypothesis that the fitness advantage of the
416 flagellar mutants resides in knocking down swimming and reducing biofilm formation which
417 may save energy that can be invested in building biomass, as previously suggested.
418

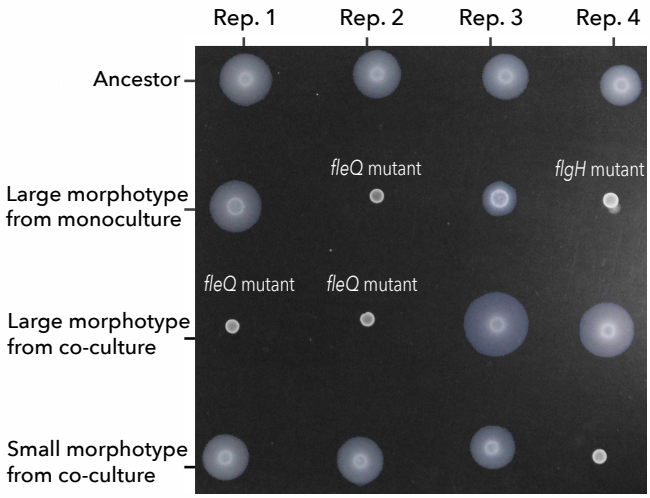

419

420 **Fig. 4. Swimming assay shows the loss of flagellar motility in the large morphotypes with**
421 **flagellar mutations.** All samples were spotted on 0.3% (w/v) FAB soft agar. The absence of a
422 halo around the initial inoculum indicates the loss of flagellum-driven motility.
423

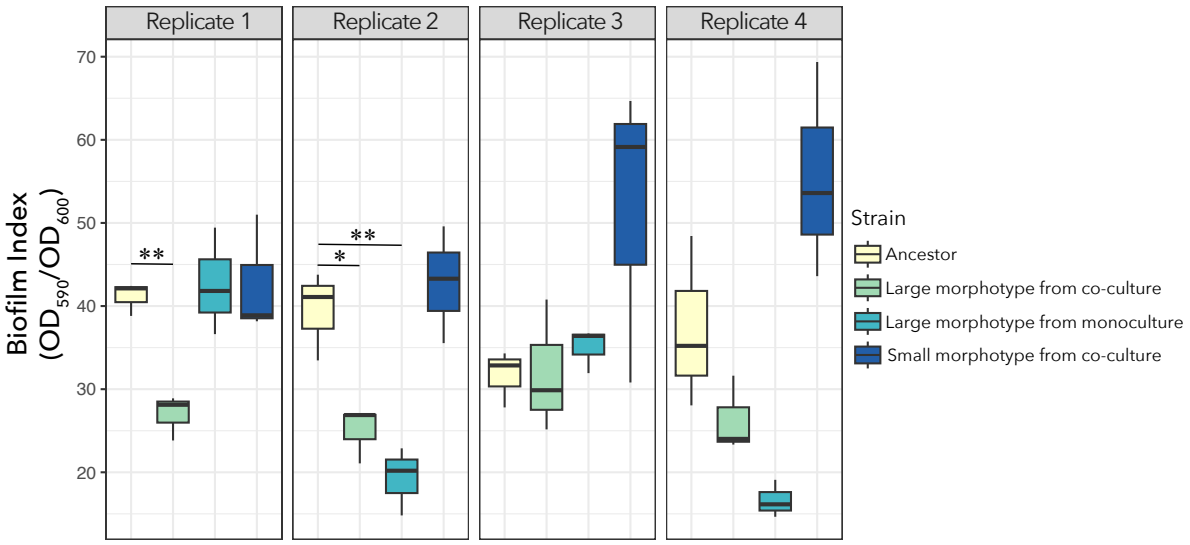

424

425 **Fig. 5. Biofilm assay shows that *fleQ* mutants produce less biofilm than the ancestor.**
426 Biofilm index (CV/OD_{600}) after a 24-hour incubation period. All *fleQ* mutants (i.e. large
427 morphotypes from co-culture replicate #1, and from the co-culture and monoculture from
428 replicate #2) had a significant reduction in the biofilm index compared to their respective
429 ancestors. Note: * = $0.01 < p < 0.05$, ** = $p < 0.01$.

430

431 **Frequency-dependent selection does not explain the coexistence of genotypes in one of the**
432 **co-cultures**

433 As previously stated, loss-of-function mutations in flagellar genes are likely to be
434 advantageous and outcompete the ancestor in monoculture conditions. Despite their fitness
435 advantage they do not sweep to fixation in populations evolved in co-culutres. We wondered if
436 the small genotypes (which are genetically different from the ancestor) have an advantage over
437 the flagellar mutations and whether this advantage is dependent on the presence of *A. johnsonii*.
438 We also wondered if coexistence is maintained by negative frequency-dependent selection. To
439 address these questions we focused on the monoculture and the co-culture populations from
440 replicate #2. In both of these populations the *fleQ* mutation is present at high frequency but it is
441 only fixed in monoculture (Fig. 3C). We performed a reciprocal invasion experiment between
442 two clones - the *fleQ* genotype and the small genotype - in the presence/absence of *A. johnsonii*.
443 The reciprocal invasion assay did not show significant differences in the rare genotypes' ability
444 to invade depending on whether *A. johnsonii* was present (Fig. S4). The small genotype tended to
445 have a higher fitness relative to the *fleQ* genotype, but these differences were not statistically
446 significant (Fig. 4, Table S2). In conclusion, these results suggest that frequency-dependent

447 selection is not a process driving coexistence between the *fleQ* and small genotypes from

448 replicate #2.

449

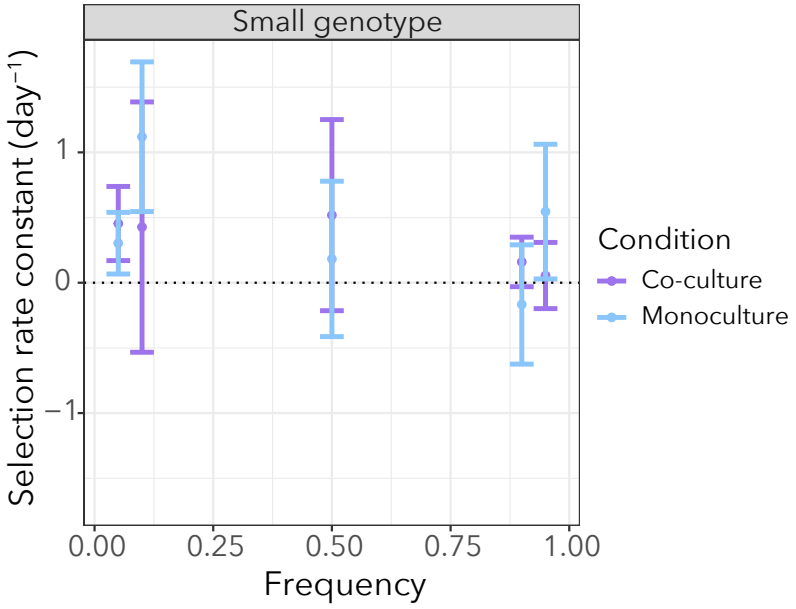

450

451 **Fig. 6. The relative growth rate of the small genotype was not affected by growth conditions**

452 **(monoculture or co-culture).** Each point shows the average of the selection rate constant and

453 the error bars represent the standard error from six replicates. Despite a tendency for the small

454 genotype to have a fitness advantage over the *fleQ* genotype (i.e., positive selection rate

455 constant), the values were not significantly different from zero (Table S2).

456

457 ***A. johnsonii* influences patterns of phenotypic diversity in co-culture**

458 In the previous section, we saw that the coexistence of the two genotypes was not

459 explained by the presence of *A. johnsonii*. It is possible that our representative genotypes did not

460 capture the stable coexistence dynamics observed at the population level. Thus, we hypothesize

461 that *A. johnsonii* plays a role in maintaining polymorphism but its effect is only captured
462 considering the entire genetic diversity. To further explore the effect of *A. johnsonii* on the
463 maintenance of phenotypic diversity (as a proxy of genotypic diversity), we did an evolutionary
464 'replay' experiment. That is, we revived the population from co-culture #2 at 138 generations
465 which was already bimorphic (Fig. 2). We then established two populations that we further
466 evolved for ~ 50 generations with and without *A. johnsonii*. We reasoned that if *A. johnsonii* is
467 important for maintaining diversity, phenotypic diversity would decline when *A. johnsonii* is
468 removed. We observed that, in the condition without *A. johnsonii*, both morphotypes gradually
469 declined but eventually recovered (Fig. 7). Interestingly, the small morphotype became dominant
470 at the end of the experiment and achieved approximately 4-fold higher density than the large
471 morphotype (two-tailed t-test, d.f. = 6, $P = 0.005$). In contrast, population densities were more
472 stable over time in the condition where *A. johnsonii* was maintained (i.e., control 'replay'
473 experiment; Fig. S5). In this condition, the large and small morphotypes achieved similar cell
474 densities, but the large morphotype achieve on average 2-fold higher density than the small
475 morphotype (two-tailed t-test, d.f. = 6, $P = 0.018$). Taken together, although we did not see the
476 extinction of one of the morphotypes when *A. johnsonii* was removed, our results suggest that *A.*
477 *johnsonii* 'buffers' population dynamics and prevent the dominance of one morphotype. The
478 mechanisms by which *A. johnsonii* influences population dynamics is an open question that
479 requires further investigation.

480

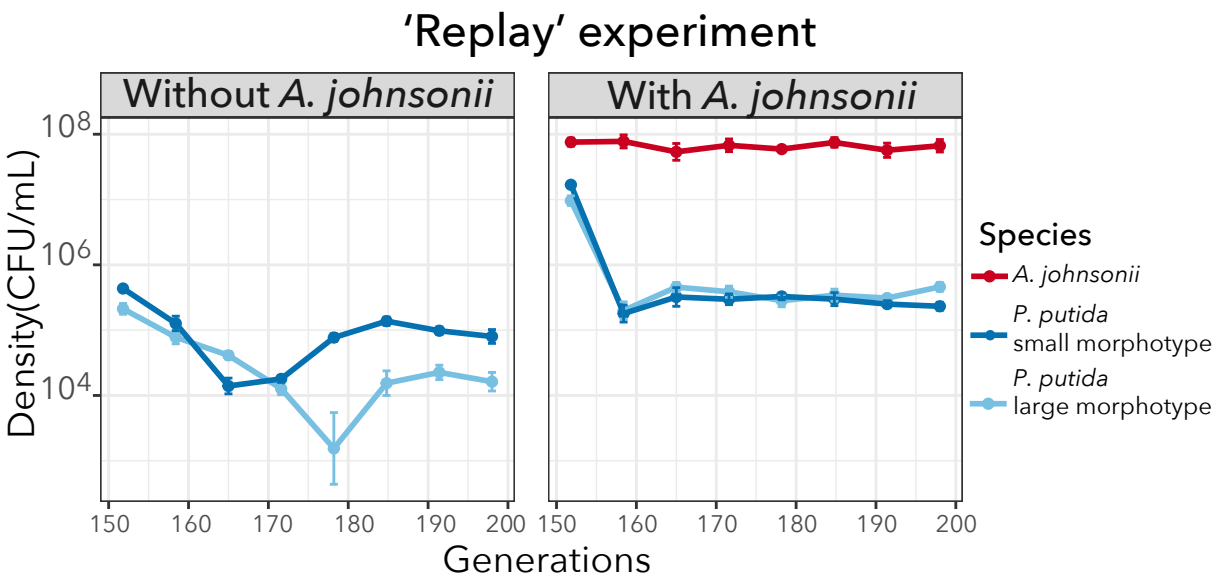

Fig. 7. *P. putida* populations dynamics were reproducible when we replayed the evolution experiment from an intermediate time point but got altered when *A. johnsonii* was removed. Mean population densities (CFU mL^{-1}) of six replicates with their standard error are represented over 50 generations. The population trajectories for each replicate are shown in Fig S5.

Discussion

The results from this study show that diversity can arise, even in a well-shaken environment with low resources. Phenotypic and genotypic diversity arose in both monoculture and co-culture conditions, however, it persisted only in co-culture conditions. This suggests that the presence of *A. johnsonii* influences evolutionary patterns.

When comparing monocultures with co-cultures, we did not observe differences in terms of the total number of mutations or proportion of nonsynonymous to synonymous mutations. This pattern agrees with other systems – e.g., *Lactobacillus plantarum* evolving with

496 *Saccharomyces cerevisiae* (20), although a higher rate of adaptation in co-culture conditions has
497 been observed in other studies (37). In our study, an interesting difference between monocultures
498 and co-cultures was that hard sweeps were only observed when *P. putida* evolved in
499 monoculture. Piccardi et al. (2024) observed a similar pattern when comparing species evolved
500 in isolation versus in a four-species community (37). They attributed hard sweeps to a sharp
501 decline in population sizes at the beginning of the experiment, which occurred only in
502 monocultures (i.e., drift). Although in our systems, population sizes in monocultures are one
503 order of magnitude lower than in co-cultures (Fig. 2), they are still large (~ 10^5 CFU/ml).
504 Therefore, we do not think that hard sweeps are attributed to drift but rather selection. We
505 showed multiple lines of evidence supporting that mutations targeting the *fleQ*, *flgH* and, *gacS*
506 genes are under strong positive selection. In addition, mutations in these genes have been
507 frequently observed in other evolution experiments using similar culture conditions (minimal
508 media and shaking environments) but with different stresses (38, 39). Thus, it is possible these
509 mutations are general adaptations to culture conditions. Flagellar mutations reducing or
510 eliminating motility have been shown to be advantageous in different culture conditions (40, 41).
511 The consensus explanation for this advantage is that the loss of flagellum motility alleviates a
512 large metabolic burden that can be invested in biomass production (30, 42). All three mutations
513 have been shown to have an effect on flagellar motility. GacS have been shown to negatively
514 regulate flagellum formation and cell motility, based on observations that *gacS* mutants are
515 highly flagellated and have greater swimming abilities (43, 44). In our study, the *gacS* mutation
516 was in the same genetic background as the *flgH* mutation (Table 1). It is possible that the two
517 mutations have opposite effects on motility, which may explain why the *flgH* mutant did not
518 fully lose motility compared to the *fleQ* mutant (Fig. 4). Importantly, regulation of cell motility

519 seems to be an important target of selection which may explain why flagellar mutations
520 outcompeted the ancestor and swept to fixation in monocultures. It is important to mention that
521 other mutations present in the populations at lower frequencies also showed improved fitness
522 (higher yield). One of these mutations was a nonsense mutation in the *uvrY* gene which is
523 homologous to *gacA*. The *gacA* gene codes the response regulator GacA of the two-component
524 system GacA/GacS and thus may be involved in the regulation of cell motility, as well (45).

525 A puzzling observation is that these mutations did not sweep to fixation in co-cultures.
526 One possibility is that clonal interference is more pronounced in co-cultures due to the larger
527 population sizes (46). That is, the *fleQ*, *flgH*, *gacS,* and *uvrY* mutations may still be advantageous
528 in co-culture conditions but they do not fix in the population because they compete with other
529 adaptive mutations. The question remains: what is the advantage of the other mutations, and
530 what is their functional relevance? One possibility is that their advantage is related to the
531 presence of *A. johnsonii,* which leaks benzoate into the medium. The excretion or leakage of
532 nutritional by-products has been shown to lead to the construction of new niches, which can
533 affect the generation and maintenance of biodiversity (47, 48). Thus, we hypothesized that *A.*
534 *johnsonii* creates transient patches of resources, and this benefits the clones that retain flagellar
535 motility and biofilm formation abilities (Fig. 3 and 4) because they are better at feeding on the
536 benzoate excreted by *A. johnsonii* (i.e., 'foraging' strategy) compared to the clones that lose their
537 ability to swim and form less biofilm. We based this hypothesis on the observation that one of
538 the small morphotypes had a 1 bp deletion in the *olpA* gene coding OlpA, the 5-oxorpolinase
539 subunit A (Table 1). Disruption of OlpA has been shown to increase surface attachment (36).
540 Furthermore, another study showed that motility increases the encounter rate between cross-
541 feeding partners and cell-cell adhesion in a well-mixed environment (49). Nevertheless, we did

542 not find support for this hypothesis when directly competing the small genotype – which retains
543 the ability to swim and form biofilms – against the *fleQ* mutant, which is unable to swim. One
544 possibility is that swimming and biofilm formation are not the traits under selection, and the
545 advantage resides in other traits. For example, *A. johnsonii* may have evolved to antagonize *P.*
546 *putida* and the small genotypes have mutations that make them resist better these selective
547 pressures. Furthermore, it is important to acknowledge that we only focused on two genotypes
548 from one replicate, which is only a subset of the whole diversity of mutations found in co-
549 cultures.

550 Our study has provided valuable insights into differences in patterns of phenotypic and
551 genotypic diversification in the presence or absence of a distantly related species. However, it is
552 important to acknowledge certain limitations in interpreting the results. First, while 200
553 generations was enough time to observe diversification, we refrain from making a definitive
554 conclusion about whether the diversity is transient (short-lived) or if it can be sustained long-
555 term. Another limitation in interpreting these results is the lack of control for the benzoate
556 excreted by *A. johnsonii*. Although benzoate was not externally supplemented to the *P. putida*
557 monocultures, they relied on residues of organic carbon present in the culture medium, i.e.,
558 assimilable organic carbon or AOC (28). Thus, an important control to discern if differences in
559 diversification patterns is only due to differences in resource concentration (e.g., impacting
560 population sizes) or can be attributed to other biotic feedbacks, future evolution experiments
561 should add an external source of benzoate to the monocultures. Such experiments would allow us
562 to determine how important it is that benzoate is produced by *A. johnsonii* (i.e., a biogenic
563 resource supply) versus being externally supplied to the medium.

564

565 **Data Availability**

566 The genome sequences have been deposited at the National Center for Biotechnology
567 Information (NCBI) Sequence Read Archive (SRA) under BioProject ID number
568 PRJNA623337. All the other data generated or analyzed during this study are included in this
569 published article and its supplemental materials.

570

571 **Acknowledgments**

572 We thank Jennifer Martiny, Brandon Gaut, and the Rodriguez-Verdugo lab members for
573 providing useful feedback during this research. This work was supported by the National Science
574 Foundation under Grant No. DEB-2234627. ARV was supported by UC Irvine's Charlie Dunlop
575 School of Biological Sciences.

576

577 **References**

578 1. **Lenski, RE, Travisano, M**. 1994. Dynamics of adaptation and diversification: a 10,000-
579 generation experiment with bacterial populations. Proc Natl Acad Sci U S A **91**:6808–6814.

580 2. **Atwood, KC, Schneider, LK, Ryan, FJ**. 1951. Periodic selection in Escherichia coli. Proc
581 Natl Acad Sci U S A **37**:146–155.

582 3. **Sniegowski, PD, Gerrish, PJ**. 2010. Beneficial mutations and the dynamics of adaptation
583 in asexual populations. Philos Trans R Soc Lond B Biol Sci **365**:1255–1263.

584 4. **Rosenzweig, RF, Sharp, RR, Treves, DS, Adams, J**. 1994. Microbial evolution in a
585 simple unstructured environment: genetic differentiation in Escherichia coli. Genetics

586 **137**:903–917.

587 5. **Friesen, ML, Saxer, G, Travisano, M, Doebeli, M**. 2004. Experimental evidence for
588 sympatric ecological diversification due to frequency-dependent competition in Escherichia
589 coli. Evolution **58**:245–260.

590 6. **Lind, PA, Farr, AD, Rainey, PB**. 2015. Experimental evolution reveals hidden diversity in
591 evolutionary pathways. Elife **4**:e07074.

592 7. **Rainey, PB, Travisano, M**. 1998. Adaptive radiation in a heterogeneous environment.
593 Nature **394**:69–72.

594 8. **Korona, R, Nakatsu, CH, Forney, LJ, Lenski, RE**. 1994. Evidence for multiple adaptive
595 peaks from populations of bacteria evolving in a structured habitat. Proc Natl Acad Sci U S
596 A **91**:9037–9041.

597 9. **Kerr, B, Riley, MA, Feldman, MW, Bohannan, BJ**. 2002. Local dispersal promotes
598 biodiversity in a real-life game of rock-paper-scissors. Nature **418**:171–174.

599 10. **Traverse, CC, Mayo-Smith, LM, Poltak, SR, Cooper, VS**. 2013. Tangled bank of
600 experimentally evolved Burkholderia biofilms reflects selection during chronic infections.
601 Proc Natl Acad Sci U S A **110**:E250–9.

602 11. **Dragoš, A, Lakshmanan, N, Martin, M, Horváth, B, Maróti, G, Falcón García, C,**
603 **Lieleg, O, Kovács, ÁT**. 2017. Evolution of exploitative interactions during diversification
604 in Bacillus subtilis biofilms. FEMS Microbiol Ecol **93**

605 12. **Rainey, PB, Buckling, A, Kassen, R, Travisano, M**. 2000. The emergence and
606 maintenance of diversity: insights from experimental bacterial populations. Trends Ecol

607 Evol **15**:243–247.

608 13. **Brisson, D**. 2018. Negative Frequency-Dependent Selection Is Frequently Confounding.
609 Front Ecol Evol **6**:10.

610 14. **Zhang, QG, Ellis, RJ, Godfray, HC**. 2012. The effect of a competitor on a model adaptive
611 radiation. Evolution **66**:1985–1990.

612 15. **Schluter, D**. 2000. The ecology of adaptative radiation., Press., OU (ed),

613 16. **Abrudan, MI, Smakman, F, Grimbergen, AJ, Westhoff, S, Miller, EL, van Wezel, GP,**
614 **Rozen, DE**. 2015. Socially mediated induction and suppression of antibiosis during
615 bacterial coexistence. Proc Natl Acad Sci U S A **112**:11054–11059.

616 17. **Leinweber, A, Fredrik Inglis, R, Kümmerli, R**. 2017. Cheating fosters species co-
617 existence in well-mixed bacterial communities. ISME J **11**:1179–1188.

618 18. **Kelsic, ED, Zhao, J, Vetsigian, K, Kishony, R**. 2015. Counteraction of antibiotic
619 production and degradation stabilizes microbial communities. Nature **521**:516–519.

620 19. **Gossmann, TI, Keightley, PD, Eyre-Walker, A**. 2012. The effect of variation in the
621 effective population size on the rate of adaptive molecular evolution in eukaryotes.
622 Genome Biol Evol **4**:658–667.

623 20. **Barber, JN, Nicholson, LC, Woods, LC, Judd, LM, Sezmis, AL, Hawkey, J, Holt, KE,**
624 **McDonald, MJ**. 2022. Species interactions constrain adaptation and preserve ecological
625 stability in an experimental microbial community. ISME J **16**:1442–1452.

626 21. **D'Souza, G, Shitut, S, Preussger, D, Yousif, G, Waschina, S, Kost, C**. 2018. Ecology
627 and evolution of metabolic cross-feeding interactions in bacteria. Nat Prod Rep **35**:455–

628 488.

629 22. **Flyvbjerg, J, Arvin, E, Jensen, BK, Olsen, SK**. 1993. Microbial degradation of phenols
630 and aromatic hydrocarbons in creosote-contaminated groundwater under nitrate-reducing
631 conditions. Journal of Contaminant Hydrology **12**:133–150.

632 23. **Møller, S, Sternberg, C, Andersen, JB, Christensen, BB, Ramos, JL, Givskov, M,**
633 **Molin, S**. 1998. In situ gene expression in mixed-culture biofilms: evidence of metabolic
634 interactions between community members. Appl Environ Microbiol **64**:721–732.

635 24. **Hansen, SK, Rainey, PB, Haagensen, JAJ, Molin, S**. 2007. Evolution of species
636 interactions in a biofilm community. Nature **445**:533–536.

637 25. **Christensen, BB, Haagensen, JA, Heydorn, A, Molin, S**. 2002. Metabolic commensalism
638 and competition in a two-species microbial consortium. Appl Environ Microbiol **68**:2495–
639 2502.

640 26. **Rodríguez-Verdugo, A**. 2021. Evolving Interactions and Emergent Functions in Microbial
641 Consortia. mSystems **6**:e0077421.

642 27. **Rodríguez-Verdugo, A, Vulin, C, Ackermann, M**. 2019. The rate of environmental
643 fluctuations shapes ecological dynamics in a two-species microbial system. Ecol Lett
644 **22**:838–846.

645 28. **Rodríguez-Verdugo, A, Ackermann, M**. 2021. Rapid evolution destabilizes species
646 interactions in a fluctuating environment. ISME J **15**:450–460.

647 29. **Deatherage, DE, Barrick, JE**. 2014. Identification of mutations in laboratory-evolved
648 microbes from next-generation sequencing data using breseq. Methods Mol Biol **1151**:165–

649 188.

650 30. **Martínez-García, E, Nikel, PI, Chavarría, M, de Lorenzo, V**. 2014. The metabolic cost
651 of flagellar motion in Pseudomonas putida KT2440. Environ Microbiol **16**:291–303.

652 31. **Ritchings, BW, Almira, EC, Lory, S, Ramphal, R**. 1995. Cloning and phenotypic
653 characterization of fleS and fleR, new response regulators of Pseudomonas aeruginosa
654 which regulate motility and adhesion to mucin. Infect Immun **63**:4868–4876.

655 32. **Zhao, L, Zhang, Q, Zhang, D**. 2016. Evolution alters ecological mechanisms of
656 coexistence in experimental microcosms. Functional Ecology **30**:1440–1446.

657 33. **Travisano, M, Lenski, RE**. 1996. Long-term experimental evolution in Escherichia coli.
658 IV. Targets of selection and the specificity of adaptation. Genetics **143**:15–26.

659 34. **Thompson, MG, Valencia, LE, Blake-Hedges, JM, Cruz-Morales, P, Velasquez, AE,**
660 **Pearson, AN, Sermeno, LN, Sharpless, WA, Benites, VT, Chen, Y, Baidoo, EEK,**
661 **Petzold, CJ, Deutschbauer, AM, Keasling, JD**. 2019. Omics-driven identification and
662 elimination of valerolactam catabolism in Pseudomonas putida KT2440 for increased
663 product titer. Metab Eng Commun **9**:e00098.

664 35. **Niehaus, TD, Elbadawi-Sidhu, M, de Crécy-Lagard, V, Fiehn, O, Hanson, AD**. 2017.
665 Discovery of a widespread prokaryotic 5-oxoprolinase that was hiding in plain sight. J Biol
666 Chem **292**:16360–16367.

667 36. **Yousef-Coronado, F, Soriano, MI, Yang, L, Molin, S, Espinosa-Urgel, M**. 2011.
668 Selection of hyperadherent mutants in Pseudomonas putida biofilms. Microbiology
669 (Reading) **157**:2257–2265.

670 37. **Piccardi, P, Ulrich, E, Garcia-Garcera, M, Martino, RD, Testa, SEA, Mitri, S**. 2024.
671 The evolution of reduced facilitation in a four-species bacterial community. Evolution
672 Letters

673 38. **Dong, F, Quevedo, AC, Wang, X, Valsami-Jones, E, Kreft, JU**. 2022. Experimental
674 evolution of Pseudomonas putida under silver ion versus nanoparticle stress. Environ
675 Microbiol **24**:905–918.

676 39. **Mohamed, ET, Werner, AZ, Salvachúa, D, Singer, CA, Szostkiewicz, K, Rafael**
677 **Jiménez-Díaz, M, Eng, T, Radi, MS, Simmons, BA, Mukhopadhyay, A, Herrgård, MJ,**
678 **Singer, SW, Beckham, GT, Feist, AM**. 2020. Adaptive laboratory evolution of
679 Pseudomonas putida KT2440 improves p-coumaric and ferulic acid catabolism and
680 tolerance. Metab Eng Commun **11**:e00143.

681 40. **Kümmerli, R, Santorelli, LA, Granato, ET, Dumas, Z, Dobay, A, Griffin, AS, West,**
682 **SA**. 2015. Co-evolutionary dynamics between public good producers and cheats in the
683 bacterium Pseudomonas aeruginosa. J Evol Biol **28**:2264–2274.

684 41. **Rodríguez-Verdugo, A, Tenaillon, O, Gaut, BS**. 2016. First-Step Mutations during
685 Adaptation Restore the Expression of Hundreds of Genes. Mol Biol Evol **33**:25–39.

686 42. **Koskiniemi, S, Sun, S, Berg, OG, Andersson, DI**. 2012. Selection-driven gene loss in
687 bacteria. PLoS Genet **8**:e1002787.

688 43. **Martínez-Granero, F, Navazo, A, Barahona, E, Redondo-Nieto, M, Rivilla, R, Martín,**
689 **M**. 2012. The Gac-Rsm and SadB signal transduction pathways converge on AlgU to
690 downregulate motility in Pseudomonas fluorescens. PLoS One **7**:e31765.

691 44. **Kim, JS, Kim, YH, Anderson, AJ, Kim, YC**. 2014. The Sensor Kinase GacS Negatively
692 Regulates Flagellar Formation and Motility in a Biocontrol Bacterium, Pseudomonas
693 chlororaphis O6. Plant Pathol J **30**:215–219.

694 45. **Song, H, Li, Y, Wang, Y**. 2023. Two-component system GacS/GacA, a global response
695 regulator of bacterial physiological behaviors. Engineering Microbiology **3**:100051.

696 46. **Lang, GI, Rice, DP, Hickman, MJ, Sodergren, E, Weinstock, GM, Botstein, D, Desai,**
697 **MM**. 2013. Pervasive genetic hitchhiking and clonal interference in forty evolving yeast
698 populations. Nature **500**:571–574.

699 47. **Callahan, BJ, Fukami, T, Fisher, DS**. 2014. Rapid evolution of adaptive niche
700 construction in experimental microbial populations. Evolution **68**:3307–3316.

701 48. **Roman, MS, Wagner, A**. 2018. An enormous potential for niche construction through
702 bacterial cross-feeding in a homogeneous environment. PLoS computational biology
703 **14**:e1006340.

704 49. **Scarinci, G, Sourjik, V**. 2023. Impact of direct physical association and motility on fitness
705 of a synthetic interkingdom microbial community. ISME J **17**:371–381.

706